J. Trop. Plant Pests Dis.
Vol. 26, No. 2, September 2026
Pages: 451–462

ISSN: 1411-7525
E-ISSN: 2461-0399
DOI : 10.23960/j.hptt.226451-462

RESEARCH PAPER

Biphasic expression pattern of heat shock protein 90 (PnHsp90) in *Pentalonia nigronervosa* during acquisition of banana bunchy top virus (BBTV)

Alan Soffan[1], Indah Nuraini[2], & Siti Subandiyah[1,2]

Manuscript received: 6 December 2024. Revision accepted: 12 December 2025. Available online: 15 July 2026

ABSTRACT

Heat shock protein 90 (Hsp90) is highly conserved molecular chaperone chaperone involved in cellular stress responses and has been implicated in insect–virus interactions. This study aimed to characterize the Hsp90 gene (PnHsp90) of *Pentalonia nigronervosa*, the principal vector of banana bunchy top virus (BBTV), and to investigate its transcriptional dynamics during virus acquisition. RNA-seq datasets (SRX6918251 and SRX6918252) were retrieved from GenBank for PnHsp90 identification and subsequent physicochemical, structural, and phylogenetic analyses using ProtParam, CYS-REC, I-TASSER, SWISS-MODEL, and MEGA X. PnHsp90 encodes a protein of 726 amino acids with an acidic theoretical isoelectric point (pI = 4.94), a high aliphatic index (82.84), and a conserved EEVD motif characteristic of cytosolic Hsp90s proteins. Structural modelling based on the *Saccharomyces cerevisiae* Hsp90–Sba1 complex (PDB: 2C9B) generated a reliable tertiary structure (TM-score = 0.72), supporting the conservation of Hsp90 domain architecture. Phylogenetic analysis placed PnHsp90 in a clade closely related to *Myzus persicae*, consistent with aphid evolutionary relationships. Quantitative real-time PCR revealed a biphasic transcriptional response during acquisition access periods (AAPs), characterized by rapid induction at 1 hour (2.5-fold), marked downregulation at 5 and 10 h, and renewed upregulation at 20 hours (1.7-fold). The dynamic expression profile suggests that PnHsp90 is involved in the physiological responses of *P. nigronervosa* during both the early and later stages of BBTV acquisition. This study provides the first integrative characterization of PnHsp90 and identifies it as a promising candidate for future functional studies aimed at elucidating the molecular mechanisms underlying BBTV acquisition and vector competence.

Keywords: Aphid–virus interaction, molecular chaperone dynamics, stress-responsive pathways, transcriptomic profiling, vector competence

INTRODUCTION

Heat shock proteins (HSPs) are evolutionarily conserved molecular chaperones that play essential roles in maintaining proteostasis and mediating cellular responses to diverse environmental stresses (Singh et al., 2024). The expression of HSPs varies across developmental stages and tissues, with the fat body typically exhibiting the highest levels (Shu et al., 2011). Based on their molecular weight, HSPs are classified into major families, including Hsp100, Hsp90, Hsp70, Hsp60, and small HSPs, and their expression is induced by heat, oxidative stress, and chemical exposure (Singh et al., 2016). Although the induction of HSPs enhances stress tolerance, excessive expression may impose physiological costs, such as reduced growth and reproduction (Sørensen et al., 2003). Among these proteins, Hsp90 is of particular importance because of its dual roles in stress adaptation and viral pathogenesis. It assists in the folding, assembly, and maturation of viral proteins, and its inhibition suppresses viral replication in several host systems (Geller et al., 2012; Lubkowska et al., 2021). In insects, Hsp90 contributes to thermal tolerance, diapause regulation, and responses to ultraviolet radiation, pesticides, and pathogens (Cheng et al., 2016; Guz et al., 2021; Shu et al., 2011; Zhao & Jones, 2012). Its involvement in viral replication has been demonstrated in diverse systems. For example, inhibition of Hsp90 suppresses *Bombyx mori* nucleopolyhedrovirus (BmNPV) proliferation through activation of the JAK/STAT pathway (Wu et al., 2019; Zhang et al., 2024), whereas in *Drosophila*, Hsp90 is required for flock house virus

Corresponding author:
Alan Soffan (alan.soffan@ugm.ac.id)

[1]Department of Plant Protection, Faculty of Agriculture, Universitas Gadjah Mada, Jl. Flora, Komplek Bulaksumur, Kocoran, Caturtunggal, Depok, Sleman, Daerah Istimewa Yogyakarta, Indonesia 55281

[2] Genetic Engineering Laboratory, Center for Biotechnology Studies, Graduate School of Universitas Gadjah Mada, Barek, Jl. Teknika Utara, Kocoran, Caturtunggal, Depok, Sleman, Daerah Istimewa Yogyakarta, Indonesia 55281

RNA polymerase synthesis and replication complex formation (Castorena et al., 2007; Kampmueller & Miller, 2005).

Although the role of Hsp90 has been extensively investigated in various insect species, information regarding the expression and function in *Pentalonia nigronervosa*, the primary vector of banana bunchy top virus (BBTV), remains limited. *P. nigronervosa* is of particular concern because it transmits BBTV, one of the most destructive banana pathogens worldwide, causing substantial yield losses and, in severe cases, total crop failure (Murhububa et al., 2023; Bagariang et al., 2019; Suparman et al., 2023). Given the pivotal role of *P. nigronervosa* in BBTV transmission and the severe impact of the disease on global banana production, understanding molecular mechanisms involving Hsp90 may provide opportunities for developing genetic- or molecular-based intervention strategies (Jekayinoluwa et al., 2021; Watanabe et al., 2015). Molecular insights into the stress- and virus-related functions of Hsp90 could therefore support the development of novel and sustainable approaches to vector management and BBTV control.

Accordingly, this study aimed to identify and characterize the Hsp90 gene of *P. nigronervosa* using RNA-seq data available in GenBank (accession numbers SRX6918251 and SRX6918252). Phylogenetic analyses were conducted to determine its evolutionary relationships with homologous sequences, and quantitative real-time reverse transcription PCR (qRT-PCR) was employed to evaluate its expression under different exposure durations to BBTV-infected banana plants. By elucidating the functional role of Hsp90 in *P. nigronervosa*, this study provides a molecular foundation for the development of RNA interference (RNAi)-based biopesticides targeting key genes involved in virus transmission. Such gene-targeting approaches could suppress aphid populations and disrupt BBTV spread, offering an innovative and environmentally sustainable strategy for banana disease management.

MATERIALS AND METHODS

Research Site. This study was conducted at the Laboratory of Genetic Engineering, Inter-University Center (PAU), and Molecular Entomology Laboratory, Universitas Gadjah Mada, Yogyakarta, Indonesia. The experimental work, including aphid rearing, BBTV acquisition assays, RNA extraction, cDNA synthesis, PCR, and qRT-PCR analyses, was carried out from August 2019 to May 2020. To incorporate advances in bioinformatics tools and improve sequence interpretation, transcriptome annotation, protein characterization, structural modeling, and phylogenetic analyses were subsequently revisited and completed in 2024. Aphid rearing and BBTV acquisition experiments were performed under controlled conditions at the insect rearing facility of the Department of Plant Protection, Faculty of Agriculture, Universitas Gadjah Mada, Yogyakarta, Indonesia.

***P. nigronervosa* Mass Rearing.** Colonies of *P. nigronervosa* were maintained on taro (*Caladium bicolor*) and banana (*Musa acuminata*) plants under controlled conditions (25 ± 2 ºC, 70 ± 10% RH, and a 12:12 h light:dark photoperiod) in an insect-proof growth chamber. BBTV-free and BBTV-infected banana plants were used as hosts for non-viruliferous and viruliferous colonies, respectively. BBTV infection in banana plants was confirmed by PCR using BBTV-R primers: F (5'-TTGAGAAACGAAAGGGRAGC-3') and R (5'-GGTGTGCGCCTGGGAAG-3'), which generated an approximately 1.1 kb amplicon (Stainton et al., 2012). Approximately 200 third-instar nymphs collected from taro plants were transferred using a fine brush to BBTV-infected banana plants. Viruliferous and non-viruliferous colonies were maintained in separate insect-proof cages to prevent cross-contamination. The viruliferous status of aphids was verified by PCR analysis.

Total RNA Extraction and cDNA Synthesis. Total RNA was extracted from pooled samples consisting of five adult *P. nigronervosa* individuals from both viruliferous and non-viruliferous colonies using the Total RNA Mini Kit (Tissue) (Geneaid, Taiwan) according to the manufacturer's instructions. Insects were homogenized using a sterile pestle prior to extraction. The extracted RNA was treated with DNase I (Thermo Scientific, USA) to remove contaminating genomic DNA. RNA concentration and purity were assessed using a MaestroGen spectrophotometer based on A260/280 and A260/230 absorbance ratios, and RNA integrity was verified by electrophoresis on a 2% agarose gel. First-strand cDNA synthesis was performed using 1 µg of total RNA and the RevertAid First Strand cDNA Synthesis Kit (Thermo Scientific, USA) with oligo(dT) primers in a 25 µL reaction volume. The synthesized cDNA was subsequently diluted to a final concentration of 100 ng/µL for qRT-PCR analysis.

PnHsp90 Primers Design. Raw RNA-seq data of

P. nigronervosa were obtained from GenBank under accession numbers SRX6918251 and SRX6918252 in FASTQ format (Subandiyah et al., 2020). De novo transcriptome assembly was performed using Trinity to generate unigenes, followed by functional annotation against the NR database to identify putative Hsp90 candidates. Differentially expressed gene (DEG) analysis was subsequently conducted using Bowtie2 for read alignment and RSEM for transcript abundance estimation. Gene expression levels were reported as fragments per kilobase of transcript per million mapped reads (FPKM).

Among the identified Hsp90 candidates, the unigene with the highest FPKM value (Unigene7683_all/PnHsp90) was selected for primer design. Primers were designed using Primer3. The primers used for PCR and qRT-PCR were PnHsp90-F (5'-GGGTCTCAATGATTGGATGG-3') and PnHsp90-R (5'-CCCTGTTGCATTGTCACATC-3'), generating a 151 bp amplicon), and PnActin-F (5'-CGGAATCATCACCAACTGGG-3') and PnActin-R (5'-GATGGCAACATACATGGCGG-3'), generating a 190 bp amplicon).

Identification of PnHsp90. The quality of *P. nigronervosa* cDNA was assessed using PCR with the universal COI primers LCO1490 (5′-GGTCAACAAATCATAAAGATATTGG-3′) and HCO2198 (5′-TAAACTTCAGGGTGACCAAAAAATCA-3′), which amplify a 710 bp fragment (Folmer et al., 1994). PCR conditions consisted of pre-denaturation at 95 ºC for 2 min, followed by 30 cycles of 95 ºC for 30 s, 50 ºC for 30 s, and 72 ºC for 1 min, with a final extension at 72 ºC for 5 min. Confirmation of the PnHsp90 gene was performed using PnHsp90-specific primers under similar conditions, except that 35 cycles were conducted with an annealing temperature of 60 ºC. All PCR reactions were performed using GoTaq Green Master Mix (Promega, USA). PCR products were visualized on 2% agarose gels stained with ethidium bromide. The PnHsp90 amplicons were subsequently purified and sequenced for molecular characterization.

Molecular Characterization of PnHsp90. Unigenes annotated as putative Hsp90 genes were retrieved from the assembled *P. nigronervosa* transcriptome and used as queries for homology searches using BLASTN and BLASTP against the NCBI database. Each nucleotide sequence was translated into its deduced amino acid sequence using the ExPASy Translate tool to identify the open reading frame (ORF).

Physicochemical properties of PnHsp90, including molecular weight, theoretical isoelectric point (pI), amino acid composition, instability index, aliphatic index, extinction coefficient, and grand average of hydropathicity (GRAVY), were calculated using ProtParam. These parameters enabled interpretation of protein stability, hydrophobicity, and charge profiles, which correspond to the biochemical characteristics reported in the Results (e.g., instability index classification, hydrophobicity, acidic residue dominance). Cysteine residues and potential disulfide-bond patterns were predicted using the CYS-REC tool to support assessment of structural stability and motif conservation.

To evaluate domain organization and structural features, three-dimensional protein models of PnHsp90 were generated using the I-TASSER suite, which predicts models through iterative threading assembly and fragment refinement. Model quality was evaluated using C-score, TM-score, and RMSD, allowing direct linkage to the structural confidence and functional relevance described in the Results (e.g., TM-score >0.5 indicating correct fold). Secondary structure composition (helix, sheet, coil) and residue-level solvent accessibility profiles were extracted from I-TASSER outputs to support the analyses of flexibility, protein–protein interaction potential, and viral protein binding capacity. Structural validation and comparative homology models were additionally produced using SWISS-MODEL.

Phylogenetic relationships between PnHsp90 and homologous insect Hsp90 proteins were inferred using amino acid sequences aligned in BioEdit v7.2 and ClustalX v2.1. Phylogenetic trees were constructed in MEGA X using the neighbor-joining method with the Poisson correction model and 1000 bootstrap replications.

PnHsp90 Gene Expressions Under Difference Acquisition Access Periods (AAPs). PnHsp90 expression dynamics were evaluated across different acquisition access periods (AAPs) of *P. nigronervosa* feeding on BBTV-infected banana plants. Prior to the experiment, aphid colonies were maintained on taro (*C. bicolor*), a non-host of BBTV, to obtain BBTV-free populations. Aphids were subsequently transferred to BBTV-infected banana plants and sampled after 0 (control), 1, 5, 10, and 20 hours of feeding.

For each AAP, three biological replicates were collected, each consisting of 10 adult aphids. Samples were preserved in RNAlater (Ambion) and subjected to total RNA extraction, followed by DNase treatment to eliminate genomic DNA contamination. First-strand

cDNA synthesis was performed from 1 µg of total RNA using the RevertAid First Strand cDNA Synthesis Kit (Thermo Scientific, USA).

Quantification of PnHsp90 expression was carried out by qRT-PCR using PowerUp™ SYBR™ Green Master Mix (Thermo Fisher Scientific, USA) on a Bio-Rad real-time PCR system. Actin was used as the internal reference gene. Each sample was analyzed in two technical replicates. Relative expression levels were calculated using the 2^–ΔΔCt method.

Data Analysis. Relative gene expression data were analyzed using the 2^{-}ΔΔCt method (Livak & Schmittgen, 2001). which quantifies relative gene expression by comparing the threshold cycle (Ct) difference between the target gene (PnHsp90) and the reference gene (PnActin). This method assumes comparable amplification efficiencies and calculates fold-change by first determining ΔCt (Ct_target – Ct_reference), followed by ΔΔCt (ΔCt_treatment – ΔCt_control), with relative expression expressed as 2^{-}ΔΔCt. Statistical differences in PnHsp90 expression across acquisition access periods (AAPs) were evaluated using one-way ANOVA, and significant pairwise differences were identified through Tukey's post hoc test. All statistical analyses were performed using SPSS version 16.0.

RESULTS AND DISCUSSION

Amino Acid of Hsp90 in *P. nigronervosa.* PnHsp90 consists of 726 amino acids with an estimated molecular weight of 83.2 kDa, and its physicochemical properties highlight several functionally relevant features (Figure 1). The theoretical isoelectric point (pI) of 4.94 indicates a strongly acidic character, supported by the greater abundance of negatively charged residues (146 Asp + Glu) compared with positively charged residues (106 Lys + Arg). This amino acid composition may influence substrate affinity and chaperone–client interactions (Blacklock & Verkhivker, 2013; Wayne & Bolon, 2010). The instability index of 44.56 classifies PnHsp90 as moderately unstable, consistent with the conformational flexibility required for dynamic protein-folding cycles (Verkhivker, 2022). Its aliphatic index of 82.84 suggests thermal adaptability, whereas the negative GRAVY value (-0.659) indicates an overall hydrophilic nature that facilitates interactions with diverse intracellular substrates (Faya et al., 2015). These combined characteristics—acidic residue predominance, moderate instability, hydrophilicity, and a high aliphatic index—are consistent with the known properties of Hsp90 proteins and support their functional role as molecular chaperones. Moreover, Hsp90 activity is regulated through post-translational modifications, including phosphorylation, which can alter conformational dynamics and client-protein interactions (Mollapour et al., 2011; Xu et al., 2019).

The deduced amino acid sequence of PnHsp90 in shown in Figure 2. As a molecular chaperone, Hsp90 plays critical roles in protein folding, stabilization, and the maintenance of cellular proteostasis. PnHsp90 possesses the characteristic domain architecture of Hsp90 proteins, consisting of an N-terminal ATP-binding domain, a middle domain involved in client-protein interactions, and a C-terminal dimerization domain (Liu et al., 2011; Yoodee et al., 2022). The sequence contains several conserved motifs that are characteristic of the Hsp90 family and are essential for interactions with a broad range of client proteins, including kinases and transcription factors (Kravats et al., 2018; Li et al., 2020; Yang et al., 2018).

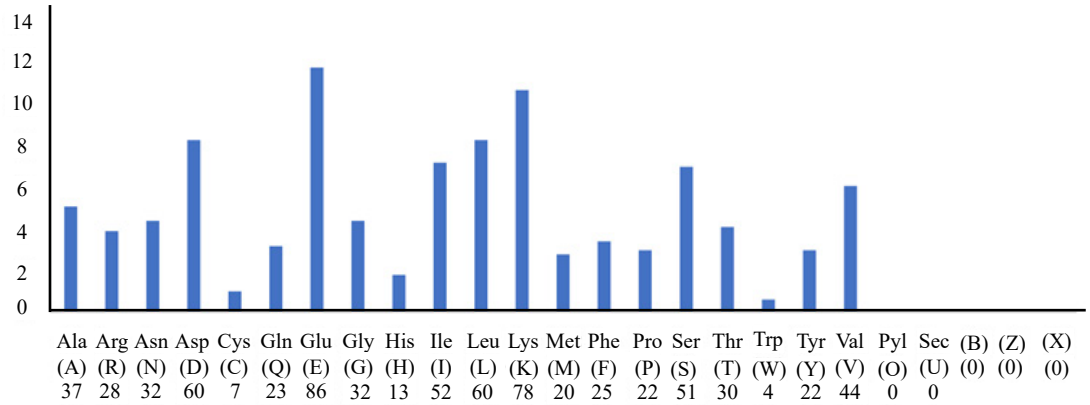

Figure 1. Amino acid composition and physicochemical characteristics of PnHsp90. The protein comprises 726 amino acids, with a predicted molecular weight of 83.24 kDa and a theoretical pI of 4.94. It contains 146 negatively charged residues (Asp + Glu) and 106 positively charged residues (Arg + Lys). The instability index, aliphatic index, and GRAVY value were 44.56, 82.84, and -0.659, respectively.

The presence of conserved amino acid residues, particularly within the C-terminal EEVD motif, is important for the binding of co-chaperones and client proteins, thereby facilitating the chaperone cycle (Chakraborty et al., 2020; Genest et al., 2013; Qiao et al., 2015). Furthermore, the overall hydrophobicity and charge distribution of PnHsp90 influence its structural stability and interaction dynamics, both of which are critical for cellular stress responses and protein homeostasis (O'Meara et al., 2019; Pratt et al., 2010). Understanding the structural and functional characteristics of Hsp90 is essential for elucidating its diverse biological roles, as this chaperone stabilizes numerous proteins involved in cellular signaling, development, and stress adaptation (Kravats et al., 2017; Taipale et al., 2012).

Protein Modelling of PnHsp90. The predicted three-dimensional structure of PnHsp90 (Figure 3) was generated using the I-TASSER server, which identified the *Saccharomyces cerevisiae* Hsp90–Sba1 co-chaperone complex (PDB ID: 2C9B) as the primary structural template. This template is widely recognized for its high-resolution representation of Hsp90 in a functional conformation, making it suitable for modeling homologous insect Hsp90 proteins. The resulting model exhibited a C-score of 0.06, an estimated TM-score of 0.72 ± 0.11, and an RMSD of 8.0 ± 4.4 Å, indicating moderate structural confidence and suggesting that the predicted fold is biologically meaningful. A TM-score greater than 0.5 generally reflects significant topological similarity to experimentally determined protein structures,

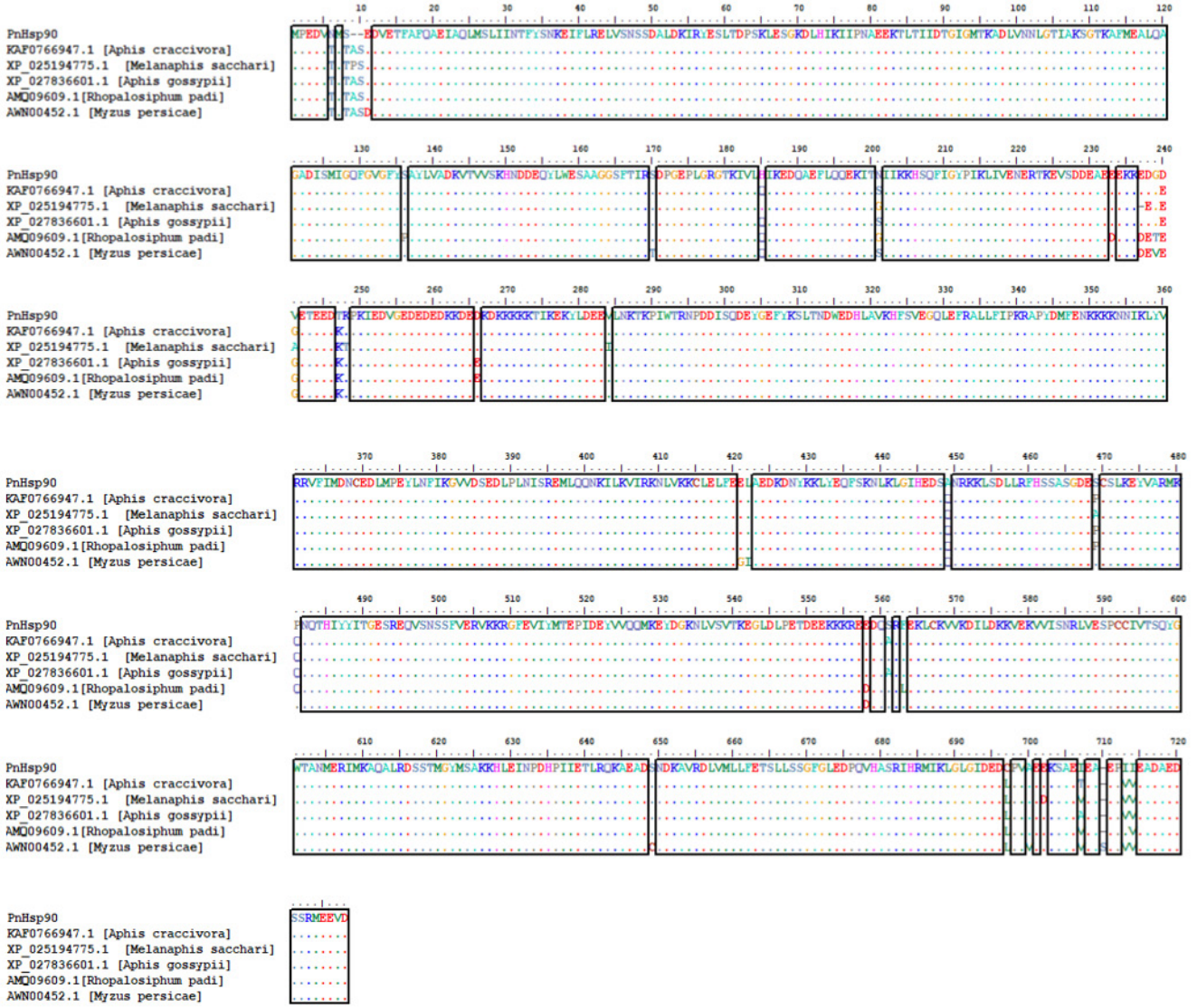

Figure 2. Deduced amino acid sequence of PnHsp90 based on open reading frame (ORF) prediction. The conserved C-terminal EEVD motif is located at the C terminus of the protein. Dots indicate amino acid residues conserved among Hsp90 homologs.

supporting the reliability of the predicted model (Blundell et al., 2017; Taipale et al., 2012).

The structural resemblance to the 2C9B Hsp90–Sba1 complex reinforces the expected domain organization of PnHsp90, including the ATP-binding N-terminal domain, the client-interacting middle domain, and the dimerization-competent C-terminal domain. This architecture underpins Hsp90's role as a molecular chaperone, particularly in stabilizing viral proteins that are often unstable without host chaperone assistance. The moderate RMSD indicates that although minor deviations from the template exist, the model sufficiently preserves key functional regions to support interactions with client proteins, including viral components (Alvira et al., 2014; Qiao et al., 2015). Such interactions are highly relevant during virus acquisition and transmission, as Hsp90 may facilitate viral protein maturation, recognition, or binding to host receptors, thereby enhancing transmission efficiency (Pascual et al., 2023; Taipale et al., 2012).

Furthermore, the structural dynamics indicated by the model may allow PnHsp90 to adapt to various client proteins, including those from viruses, thereby playing a pivotal role in the lifecycle of plant pathogens transmitted by insects (Street et al., 2011). Thus, the structural characteristics of PnHsp90, as revealed by the model, correlate closely with its functional role in mediating plant virus transmission.

The predicted secondary structure of PnHsp90 consisted of approximately 42.21% random coils, 41.52% α-helices, and 16.28% β-strands. The predominance of coils and α-helices suggests a flexible and adaptable protein structure, which is characteristic of molecular chaperones and supports their ability to interact with a broad range of client proteins (García-Gómez et al., 2019; Wojda & Kowalski, 2013). Although less abundant, β-strands may contribute to the structural stability of protein complexes formed during these interactions. Collectively, this secondary structure composition is consistent with the functional properties reported for Hsp90 proteins in other organisms.

Analysis of solvent accessibility revealed a heterogeneous distribution of exposed and buried residues across the PnHsp90 structure. The high proportion of residues with an accessibility score of 0 (240 residues) suggests that a substantial portion of the protein forms a structurally stable core, which is typical

A

```
PnHsp90                 NMPEDVNMSEDVETFAFQAEIAQLMSLIINTFYSNKEIFLRELVSNSSDALDKIRYESLTDPSKLESGKD
Secondary Structure     CCCCCCCCCCCCSSSSSHHHHHHHHHHHHCCCCCHHHHHHHHHHHHHHHHHHHHHCCCCHHCCCCCC
solvent acessability    836544524654442413230330030003001021000000000000000010102102364235746 4

PnHsp90                 LHIKIIPNAEEKTLTIIDTGIGMTKADLVNNLGTIAKSGTKAFMEALQAGADISMIGQFGVGFYSAYLVA
Secondary Structure     CSSSSSSCCCCCSSSSSSCCCCCCHHHHHHCCSSSSSCCHHHHHHHHHCCCCCCCCCCCCHHHHHHHHCC
solvent acessability    030202114763001020100002361026101100210044015304644443000001110100000 0

PnHsp90                 DKVTVVSKHNDDEQYLWESAAGGSFTIRSDPGEPLGRGTKIVLHIKEDQAEFLQQEKITNIIKKHSQFIG
Secondary Structure     CSSSSSSSCCCCCCSSSSSSCCCCSSSSSCCCCCCCCCCSSSSSSCCCCHHHCCHHHHHHHHHHHCCCC
solvent acessability    330102022363500201041634020341666413110300000143243103432034103003100 0

PnHsp90                 YPIKLIVENERTKEVSDDEAEEEKKEDGDVETEEDTKPKIEDVGEDEDEDKKDEDKDKKKKKTIKEKYLD
Secondary Structure     CCSSSSSCCCCCCCCCCCCCCCCCCCCCCCCCCSSSCCCCCCCCCCHHHHCCCHHHHHHCCCCCSSSSSSCC
solvent acessability    000101144444342444444444554444444545454444444464444455464464543444334 0

PnHsp90                 EEVLNKTKPIWTRNPDDISQDEYGEFYKSLTNDWEDHLAVKHFSVEGQLEFRALLFIPKRAPYDMFENKK
Secondary Structure     CHHCCCCCCCCCCCCCCCCCHHHHHHHHHHHCCCCCCCSSSSSSCCCCCCSSSSSSSSCCCCCHHHHHHHC
solvent acessability    233016331203243741466303400343133243000000020323130300000053002100235 6

PnHsp90                 KKNNIKLYVRRVFIMDNCEDLMPEYLNFIKGVVDSEDLPLNISREMLQQNKILKVIRKNLVKKCLELFEE
Secondary Structure     CCCCHHHHHHHHHHHCCHHHHCCHHHHHHSSSSSCCCCCCCCCHHHHCCCHHHHHHHHHHHHHHHHHHH
solvent acessability    353101000120002330340013002000000207301020124203534103302430031014005 4

PnHsp90                 LAEDKDNYKKLYEQFSKNLKLGIHEDSANRKKLSDLLRFHSSASGDESCSLKEYVARMKPNQTHIYYITG
Secondary Structure     HHHHHHHHHHHHHHHHHHHHHSSSSCCHHHHHHHHHHHSSSSCCCCCCSSSHHHHHHCCCCCCSSSSSSS
solvent acessability    036346303300530031000000204601630140010000437633010420064047523200000 0

PnHsp90                 ESREQVSNSSFVERVKKRGFEVIYMTEPIDEYVVQQMKEYDGKNLVSVTKEGLDLPETDEEKKKREEDQS
Secondary Structure     CCHHHHHHCHHHHHHHHCCCSSSSSCCCHHHHHHHHHHHHCCCCSSSSSCCCCCCCCCCHHHHHHHHHH
solvent acessability    312620360310230363400000000300000031045157140220035415156565445455345 5

PnHsp90                 RFEKLCKVVKDILDKKVEKVVISNRLVESPCCIVTSQYGWTANMERIMKAQALRDSSTMGYMSAKKHLEI
Secondary Structure     HHHHHHHHHHHHHHCCCCSSSSSSCCCCCCCCCCCCCHHHHHHHHHHHHHHCCCCCCCCCCCCCSSSSS
solvent acessability    414400420261066414403014203410000001322103301320342434344444223332000 0

PnHsp90                 NPDHPIIETLRQKAEADSNDKAVRDLVMLLFETSLLSSGFGLEDPQVHASRIHRMIKLGLGIDEDCPVAE
Secondary Structure     CCCCHHHHHHHHHHCCCHHHHHHHHHHHHHHHHHHCCCCCCCHHHHHHHHHHHHHHHCCCCCCCCCCCC
solvent acessability    005130043026316636426303300200000000214040720440041003003300614464635 5

PnHsp90                 EKSAEIEAEPIIEADAEDSSRMEEVD
Secondary Structure     CCCCCCCCCCCCCCCCCCCCCCCCC
solvent acessability    464554654444564464454346 38
```

B

Figure 3. Structure model of PnHsp90 predicted using I-TASSER. A. Secondary structure organization comprising α-helices (H, red), β-sheets (S, yellow), and loop (C-green); B. Confidence score for secondary structure prediction and solvent accessibility analysis. Solvent accessibility values range from 0, representing buried residues, to 9, representing highly exposed residues.

of regions involved in maintaining protein integrity and mediating intramolecular interactions (Graf et al., 2014; Zhang et al., 2015). In contrast, residues with higher accessibility scores, particularly scores 3 and 4, represent surface-exposed regions that may participate in interactions with client proteins, co-chaperones, or other cellular components (Yoshimura et al., 2021).

These solvent-accessible regions are likely important for the chaperone function of PnHsp90 because they provide potential binding interfaces required for client-protein recognition and stabilization (Tsutsumi et al., 2012). The relatively low frequency of highly exposed residues (scores 8 and 9) further indicates that most of the protein structure is optimized for stability while maintaining sufficient surface accessibility for functional interactions (Blacklock & Verkhivker, 2013). Overall, the solvent accessibility profile supports the structural characteristics expected of a functional Hsp90 molecular chaperone and provides a foundation for future investigations into its biological roles in *P. nigronervosa*.

Phylogenetic Analysis of PnHsp90. Phylogenetic analysis of the Hsp90 gene was conducted using the General Time Reversible model with gamma distribution (GTR+G). The resulting phylogenetic tree showed that PnHsp90 from *P. nigronervosa* clustered closely with *Myzus persicae*, indicating a relatively close evolutionary relationship between these two aphid species (Figure 4). Both species formed a distinct clade, suggesting that their Hsp90 genes originated from a more recent common ancestor. In contrast, *S. litura* formed a separate but related cluster, indicating a greater evolutionary distance from the aphid clade. The *Dendrolimus* species were positioned more distantly in the tree, suggesting a much earlier divergence from the common ancestor shared by *P. nigronervosa* and *M. persicae*.

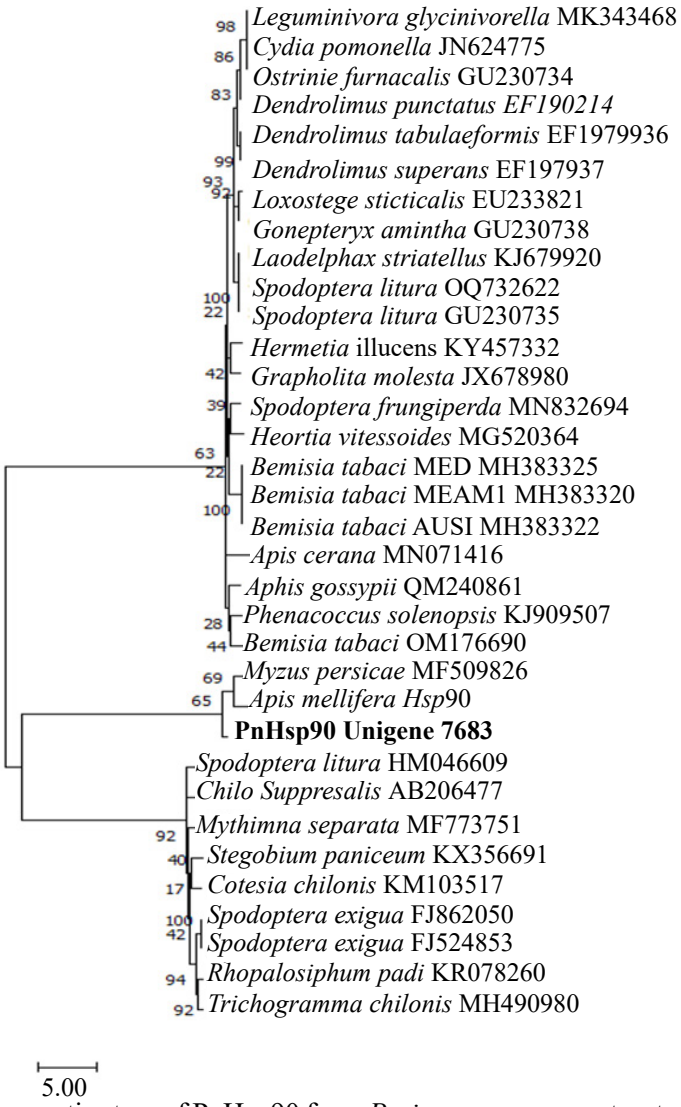

Figure 4. Molecular phylogenetics tree of PnHsp90 from *P. nigronervosa* constructed using the best-fit substitution model GTR+G.

The phylogenetic relationships observed in this study indicate that the evolutionary history of Hsp90 generally follows taxonomic relationships among insect species, with aphid species exhibiting higher sequence conservation than more distantly related lepidopteran insects. The close clustering of *P. nigronervosa* and *M. persicae* suggests that Hsp90 may perform conserved physiological functions in aphids, including roles in cellular homeostasis and stress responses.

PnHsp90 Expression Dynamics Across Acquisition Access Periods (AAPs). The temporal expression profile of PnHsp90 was evaluated in *P. nigronervosa* following acquisition access periods (AAPs) of 0, 1, 5, 10, and 20 hours on BBTV-infected banana plants using using qRT-PCR. Actin was used as the reference gene for normalization because it is widely employed as a constitutively expressed housekeeping gene in insect gene expression studies.

PnHsp90 exhibited a biphasic expression pattern during the acquisition period (Figure 5). At 1 hour AAP, PnHsp90 transcript abundance increased approximately 2.5-fold relative to the 0 hour control, indicating rapid transcriptional activation shortly after exposure to BBTV-infected tissue. This early induction suggests that PnHsp90 participates in the initial cellular response associated with virus acquisition and feeding on infected plants.

Expression subsequently declined to approximately 0.5-fold and 0.2-fold at 5 hours and 10 hours AAP, respectively, indicating significant downregulation following the initial induction phase. This decrease may reflect physiological adjustment during prolonged feeding or modulation of the early stress response. At 20 hours AAP, PnHsp90 expression increased again to approximately 1.7-fold relative to the control, indicating a secondary activation phase.

Overall, the observed pattern, characterized by early induction, intermediate suppression, and late reactivation, suggests that PnHsp90 is dynamically regulated during BBTV acquisition. Similar fluctuations in Hsp90 expression have been reported in other insect–virus systems, where Hsp90 is implicated in cellular stress responses and virus–vector interactions (Wu et al., 2016). Although the precise role of PnHsp90 during BBTV acquisition remains to be elucidated, the present findings indicate that this gene may be involved in the physiological responses of *P. nigronervosa* during virus acquisition and warrants further functional characterization using gene-silencing or genome-editing approaches (RNAi, CRISPR, or other molecular intervention strategies).

CONCLUSION

This study presents the first molecular characterization of Hsp90 in *Pentalonia nigronervosa* and provides evidence of its dynamic regulation during BBTV acquisition. PnHsp90 possesses conserved Hsp90 structural featurescharacteristic of the Hsp90 family, including an acidic amino acid-rich composition and a secondary structure compatible with its molecular chaperone function. Protein modeling further supported the formation of a biologically relevant three-dimensional structure. Expression analysis revealed a biphasic pattern of PnHsp90 regulation, characterized by early induction, mid-phase suppression, and late reactivation during acquisition access periods on BBTV-infected plants. These temporal changes suggest that PnHsp90 may participate in the physiological responses of P. nigronervosa associated with virus acquisition and

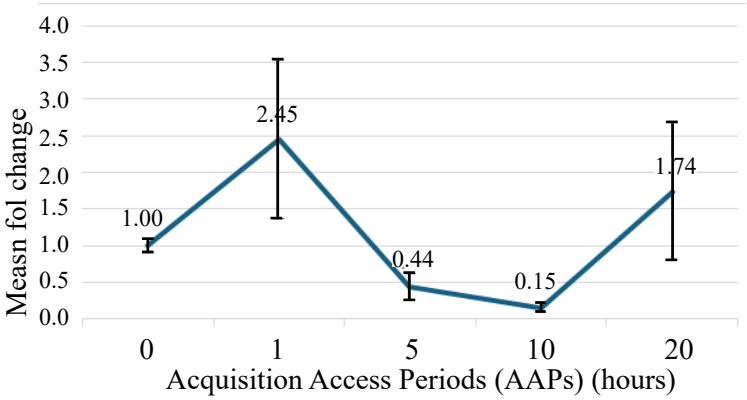

Figure 5. Relative expression of the PnHsp90 gene in *P. nigronervosa* following different acquisition access periods (AAPs) of 0, 1, 5, 10, and 20 hours on BBTV-infected banana plants. Gene expression levels were quantified by qRT-PCR using actin as the reference gene.

adaptation to feeding on infected tissues. Although the precise functional role of PnHsp90 in BBTV transmission remains to be elucidated, the present findings identify this gene as a promising candidate for future functional studies and potential molecular interventions, including RNA interference (RNAi) and CRISPR-based approaches aimed at reducing vector competence and supporting sustainable BBTV management.

ACKNOWLEDGMENTS

The authors gratefully acknowledge the facilities and technical support provided by the Genetic Engineering Laboratory and the Molecular Entomology Laboratory, Department of Plant Protection, Faculty of Agriculture, Universitas Gadjah Mada. This research was supported by the Bill & Melinda Gates Foundation (Grant ID: OPP1130226) and the Asistensi Riset 2024 Progam 2024. The authors also thank Vindi Septia Putri for her valuable assistance with laboratory experiments and sample processing.

FUNDING

This research was funded by the Bill & Melinda Gates Foundation (Grant ID: OPP1130226) and supported by the Asistensi Riset Program 2024, Universitas Gadjah Mada.

AUTHORS' CONTRIBUTIONS

AS conceived and designed the study, developed the methodology, validated the results, supervised the research activities, prepared the original draft, and reviewed and edited the manuscript. IN conducted the experiments, curated and analyzed the data, and contributed to manuscript preparation. SS conceived the study, secured funding, supervised the research, and reviewed and edited the manuscript. All authors read and approved the final version of the manuscript.

COMPETING INTEREST

The authors declare that they have no competing interests.

REFERENCES

Alvira S, Cuéllar J, Röhl A, Yamamoto S, Itoh H, Alfonso C, Rivas G, Büchner J, & Valpuesta JM. 2014. Structural characterization of the substrate transfer mechanism in Hsp70/Hsp90 folding machinery mediated by Hop. *Nat. Commun*. 5(1): 5484. https://doi.org/10.1038/ncomms6484

Bagariang W, Hidayat P, & Hidayat SH. 2019. Morphometric analysis and host range of the genus *Pentalonia* Coquerel (Hemiptera: Aphididae) infesting banana in Java. *Indones. J. Plant Prot*. 23(2): 171–178. https://doi.org/10.22146/jpti.38220

Blacklock K & Verkhivker GM. 2013. Experimentally guided structural modeling and dynamics analysis of Hsp90–p53 interactions: Allosteric regulation of the Hsp90 chaperone by a client protein. *J. Chem. Inf. Model*. 53(11): 2962–2978. https://doi.org/10.1021/ci400434g

Blundell KLIM, Pal M, Roe SM, Pearl LH, & Prodromou C. 2017. The structure of FKBP38 in complex with the MEEVD tetratricopeptide binding motif of Hsp90. *PLoS One*. 12(3): e0173543. https://doi.org/10.1371/journal.pone.0173543

Castorena KM, Weeks SA, Stapleford KA, Cadwallader AM, & Miller DJ. 2007. A functional heat shock protein 90 chaperone is essential for efficient flock house virus RNA polymerase synthesis in *Drosophila* cells. *J. Virol*. 81(16): 8412–8420. https://doi.org/10.1128/jvi.00189-07

Chakraborty A, Boel NME, & Edkins AL. 2020. Hsp90 interacts with the fibronectin N-terminal domains and increases matrix formation. *Cells*. 9(2): 272. https://doi.org/10.3390/cells9020272

Cheng W, Li D, Wang Y, Liu Y, & Zhu-Salzman K. 2016. Cloning of heat shock protein genes (hsp70, hsc70 and hsp90) and their expression in response to larval diapause and thermal stress in the wheat blossom midge, *Sitodiplosis mosellana. J. Insect Physiol.* 95: 66–77. https://doi.org/10.1016/j.jinsphys.2016.09.005

Faya N, Penkler DL, & Bishop ÖT. 2015. Human, vector and parasite Hsp90 proteins: A comparative bioinformatics analysis. *FEBS Open Bio*. 5(1): 916–927. https://doi.org.10.1016/j.fob.2015.11.003

Folmer O, Black M, Hoeh W, Lutz R. & Vrijenhoek, R. 1994. DNA primers for amplification of mitochondrial cytochrome c oxidase subunit I

from diverse metazoan invertebrates. *Mol. Mar. Biol. Biotechnol.*3(5): 294–299.

García-Gómez BI, Cano SN, Zagal EE, Dantán-González E, Bravo A, & Soberón M. 2019. Insect Hsp90 chaperone assists *Bacillus thuringiensis* Cry toxicity by enhancing protoxin binding to the receptor and by protecting protoxin from gut protease degradation. *MBio*. 10(6): 10–128. https://doi.org/10.1128/mBio.02775-19

Geller R, Taguwa S, & Frydman J. 2012. Broad action of Hsp90 as a host chaperone required for viral replication. *Biochim. Biophys. Acta - Mol. Cell Res*. 1823(3): 698–706. https://doi.org/10.1016/j.bbamcr.2011.11.007

Genest O, Reidy M, Street TO, Hoskins JR, Camberg JL, Agard DA, Masison DC, & Wickner S. 2013. Uncovering a region of heat shock protein 90 important for client binding in *E. coli* and chaperone function in yeast. *Mol. Cell.* 49(3): 464–473. https://doi.org/10.1016/j.molcel.2012.11.017

Graf C, Lee CT, Meier-Andrejszki LE, Nguyen MTN, & Mayer MP. 2014. Differences in conformational dynamics within the Hsp90 chaperone family reveal mechanistic insights. *Front. Mol. Biosci.* 1: 4. https://doi.org/10.3389/fmolb.2014.00004

Guz N, Dageri A, Altincicek B, & Aksoy S. 2021. Molecular characterization and expression patterns of heat shock proteins in *Spodoptera littoralis*, heat shock or immune response? *Cell Stress Chaperones*. 26(1): 29–40. https://doi.org/10.1007/s12192-020-01149-2

Jekayinoluwa T, Tripathi JN, Dugdale B, Obiero G, Muge E, Dale JL, & Tripathi L. 2021. Transgenic expression of dsRNA targeting the *Pentalonia nigronervosa* acetylcholinesterase gene in banana and plantain reduces aphid populations. *Plants*. 10(4): 613. https://doi.org/10.3390/plants10040613

Kampmueller KM & Miller DJ. 2005. The cellular chaperone heat shock protein 90 facilitates Flock House virus RNA replication in *Drosophila* cells. *J. Virol.* 79(11): 6827–6837. https://doi.org/10.1128/jvi.79.11.6827-6837.2005

Kravats AN, Doyle SM, Hoskins JR, Genest O, Doody E, & Wickner S. 2017. Interaction of *E. coli* Hsp90 with DnaK involves the DnaJ binding region of DnaK. *J. Mol. Biol*. 429(6): 858–872. https://doi.org/10.1016/j.jmb.2016.12.014

Kravats AN, Hoskins JR, Reidy M, Johnson JL, Doyle SM, Genest O, Masison DC, & Wickner S. 2018. Functional and physical interaction between yeast Hsp90 and Hsp70. *PNAS*. 115(10): E2210–E2219. https://doi.org/10.1073/pnas.1719969115

Li K, Sun P, Wang Y, Gao T, Zheng D, Liu A, & Ni Y. 2020. Hsp90 interacts with Cdc37, is phosphorylated by PKA/PKC, and regulates SRC phosphorylation in human sperm capacitation. *Andrology*. 9(1): 185–195. https://doi.org/10.1111/andr.12862

Liu T, Hou X, Zhang J, Song Y, Zhang S, & Liu Y. 2011. A cDNA clone of BcHSP81-4 from the sterility line (Pol CMS) of non-heading Chinese cabbage (*Brassica campestri*s ssp. *chinensis*). *Plant Mol. Biol. Rep.* 29(3): 723–732. https://doi.org/10.1007/s11105-010-0285-y

Livak KJ & Schmittgen TD. 2001. Analysis of relative gene expression data using real-time quantitative PCR and the 2^−ΔΔCt method. *Methods*. 25(4): 402–408. https://doi.org/10.1006/meth.2001.1262

Lubkowska A, Pluta W, Strońska A, & Lalko A. 2021. Role of heat shock proteins (HSP70 and HSP90) in viral infection. *Int. J. Mol. Sci*. 22(17): 9366. https://doi.org/10.3390/ijms22179366

Mollapour M, Tsutsumi S, Kim YS, Trepel JB, & Neckers L. 2011. Casein kinase 2 phosphorylation of Hsp90 threonine 22 modulates chaperone function and drug sensitivity. *Oncotarget*. 2(5): 407–417. https://doi.org/10.18632/oncotarget.272

Murhububa IS, Tougeron K, Bragard C, Fauconnier ML, Bugeme DM, Basengere EB, Masamba JW, & Hance T. 2023. The aphid *Pentalonia nigronervosa* (Hemiptera: Aphididae) takes advantage from the quality change in banana plant associated with banana bunchy top virus infection. *J. Econ. Entomol.* 116(5): 1481–1489. https://doi.org/10.1093/jee/toad130

O'Meara TR, O'Meara MJ, Polvi EJ, Pourhaghighi MR, Liston SD, Lin ZY, Veri AO, Emili A, Gingras AC, & Cowen LE. 2019. Global proteomic analyses define an environmentally contingent Hsp90 interactome and reveal chaperone-dependent regulation of stress

granule proteins and the R2TP complex in a fungal pathogen. *PLoS Biol.* 17(7): e3000358. https://doi.org/10.1371/journal.pbio.3000358

Pascual S, Rodríguez-Álvarez CI, Kaloshian I, & Nombela G. 2023. *Hsp90* gene is required for *Mi-1*-mediated resistance of tomato to the whitefly *Bemisia tabaci. Plants.* 12(3): 641. https://doi.org/10.3390/plants12030641

Pratt WB, Morishima Y, Peng HM, & Osawa Y. 2010. Proposal for a role of the Hsp90/Hsp70-based chaperone machinery in making triage decisions when proteins undergo oxidative and toxic damage. *Exp. Biol. Med.* 235(3): 278–289. https://doi.org/10.1258/ebm.2009.009250

Qiao L, Wu J, Qin DZ, Liu XC, Lu ZC, Lv L, Pan ZL, Chen H, & Li GW. 2015. Gene expression profiles of heat shock proteins 70 and 90 from *Empoasca onukii* (Hemiptera: Cicadellidae) in response to temperature stress. *J. Insect Sci.* 15(1): 49. https://doi.org/10.1093/jisesa/iev030

Shu Y, Du Y, & Wang J. 2011. Molecular characterization and expression patterns of *Spodoptera litura* heat shock protein 70/90, and their response to zinc stress. *Comp. Biochem. Physiol. A Mol. Integr. Physiol.* 158(1): 102–110. https://doi.org/10.1016/j.cbpa.2010.09.006

Singh A, Puri D, Kumar B, & Singh SK. 2016. Heat shock proteins: Knowledge so far and its future prospects. *Asian J. Pharm. Clin. Res*. 9(5): 1–8.

Singh MK, Shin Y, Ju S, Han S, Choe W, Yoon K-S, Kim SS, & Kang I. 2024. Heat shock response and heat shock proteins: Current understanding and future opportunities in human diseases. *Int. J. Mol. Sci.* 25(8): 4209. https://doi.org/10.3390/ijms25084209

Sørensen JG, Kristensen TN, & Loeschcke V. 2003. The evolutionary and ecological role of heat shock proteins. *Ecol. Lett.* 6(11): 1025–1037. https://doi.org/10.1046/j.1461-0248.2003.00528.x

Stainton D, Kraberger S, Walters M, Wiltshire EJ, Rosario K, Halafihi M, Lolohea S, Katoa I, Faitua TH, Aholelei W, Taufa L, Thomas JE, Collings DA, Martin DP, & Varsani1 A. 2012. Evidence of inter-component recombination, intra-component recombination and reassortment in banana bunchy top virus. *J. Gen. Virol*. 93(5): 1103–1119. https://doi.org/10.1099/vir.0.040337-0

Street TO, Lavery LA, & Agard DA. 2011. Substrate binding drives large-scale conformational changes in the Hsp90 molecular chaperone. *Mol. Cell.* 42(1): 96–105. https://doi.org/10.1016/j.molcel.2011.01.029

Subandiyah S, Rahayuniati RF, Hartono S, Somowiyarjo S, Afiahayati & Soffan A. 2020. RNA-seq data of banana bunchy top virus (BBTV) viruliferous and non-viruliferous banana aphid (*Pentalonia nigronervosa*). *Data Br*. 28: 104860. https://doi.org/10.1016/j.dib.2019.104860

Suparman, Oktarida R, Hamidson H, & Arsi. 2023. Morphometrics and biological characteristics of *Pentalonia nigronervosa*, the vector of banana bunchy top virus, living on various Araceous plant species. *J. Trop. Plant Pests Dis.* 23(1): 77–87. https://doi.org/10.23960/jhptt.12377-87

Taipale M, Krykbaeva I, Koeva M, Kayatekin C, Westover KD, Karras GI, & Lindquist S. 2012. Quantitative analysis of Hsp90-client interactions reveals principles of substrate recognition. *Cell*. 150(5): 987–1001. https://doi.org/10.1016/j.cell.2012.06.047

Tsutsumi S, Mollapour M, Prodromou C, Lee CT, Panaretou B, Yoshida S, Mayer MP, & Neckers LM. 2012. Charged linker sequence modulates eukaryotic heat shock protein 90 (Hsp90) chaperone activity. *PNAS.* 109(8): 2937–2942. https://doi.org/10.1073/pnas.1114414109

Verkhivker GM. 2022. Conformational dynamics and mechanisms of client protein integration into the Hsp90 chaperone controlled by allosteric interactions of regulatory switches: Perturbation-based network approach for mutational profiling of the Hsp90 binding and allostery. *J. Phys. Chem. B.* 126(29): 5421–5442. https://doi.org/10.1021/acs.jpcb.2c03464

Watanabe S, Borthakur D, & Bressan A. 2015. Localization of banana bunchy top virus and cellular compartments in gut and salivary gland tissues of the aphid vector *Pentalonia nigronervosa. Insect Sci.* 23(4): 591–602. https://doi.org/10.1111/1744-7917.12211

Wayne N & Bolon DN. 2010. Charge-rich regions modulate the anti-aggregation activity of Hsp90. *JMB*. 401(5): 931–939. https://doi.org/10.1016/j.jmb.2010.06.066

Wojda I & Kowalski P. 2013. *Galleria mellonella*

infected with *Bacillus thuringiensis* involves Hsp90. *Cent. Eur. J. Biol.* 8(6): 561–569. https://doi.org/10.2478/s11535-013-0162-9

Wu P, Jiang X, Guo X, Li L, & Chen T. 2016. Genome-wide analysis of differentially expressed microRNA in *Bombyx mori* infected with nucleopolyhedrosis virus. *PLoS One*. 11(11): e0165865. https://doi.org/10.1371/journal.pone.0165865

Wu P, Shang Q, Huang H, Zhang S, Zhong J, Hou Q, & Guo X. 2019. Quantitative proteomics analysis provides insight into the biological role of Hsp90 in BmNPV infection in *Bombyx mori. J. Proteom.* 203: 103379. https://doi.org/10.1016/j.jprot.2019.103379

Xu W, Beebe K, Chavez JD, Boysen M, Lu Y, Zuehlke AD, Keramisanou D, Trepel JB, Prodromou C, Mayer M, Bruce JE, Gelis I, & Neckers L. 2019. Hsp90 middle domain phosphorylation initiates a complex conformational program to recruit the ATPase-stimulating cochaperone Aha1. *Nat. Commun.* 10(1): 2574. https://doi.org/10.1038/s41467-019-10463-y

Yang Y, Wang W, Li M, Gao Y, Zhang W, Huang Y, Zhuo W, Yan X, Liu W, Wang F, Chen D, & Zhou T. 2018. NudCL2 is an Hsp90 cochaperone to regulate sister chromatid cohesion by stabilizing cohesin subunits. *Cell. Mol. Life Sci.* 76(2): 381–395. https://doi.org/10.1007/s00018-018-2957-y

Yoodee S, Peerapen P, Plumworasawat S, & Thongboonkerd V. 2022. Roles of heat-shock protein 90 and its four domains (N, LR, M and C) in calcium oxalate stone-forming processes. *Cell. Mol. Life Sci.* 79(8): 454. https://doi.org/10.1007/s00018-022-04483-z

Yoshimura C, Nagatoishi S, Kuroda D, Kodama Y, Uno T, Kitade M, Chong-Takata K, Oshiumi H, Muraoka H, Yamashita S, Kawai Y, Ohkubo S, & Tsumoto K. 2021. Thermodynamic dissection of potency and selectivity of cytosolic Hsp90 inhibitors. *J. Med. Chem.* 64(5): 2669–2677. https://doi.org/10.1021/acs.jmedchem.0c01715

Zhang H, Zhou C, Chen W, Xu Y, Shi Y, Wen Y, & Zhang N. 2015. A dynamic view of ATP-coupled functioning cycle of Hsp90 N-terminal domain. *Sci. Rep.* 5(1): 9542. https://doi.org/10.1038/srep09542

Zhang X, Ma S, Gu C, Hu M, Miao M, Quan Y, & Yu W. 2024. K64 acetylation of heat shock protein 90 suppresses nucleopolyhedrovirus replication in *Bombyx mori. Arch. Insect Biochem. Physiol.* 115(1): e22079. https://doi.org/10.1002/arch.22079

Zhao L & Jones WA. 2012. Expression of heat shock protein genes in insect stress responses. *Invert. Surviv. J.* 9(1): 93–101.